

Magnetic-resonance imaging of the human brain with an atomic magnetometer

I. Savukov¹ and T. Karaulanov²

¹Los Alamos National Laboratory, Los Alamos, New Mexico 87545, USA

²CNLS-Los Alamos National Laboratory, Los Alamos, New Mexico 87545, USA

(Received 6 June 2013; accepted 5 July 2013; published online 23 July 2013)

Magnetic resonance imaging (MRI) is conventionally performed in very high fields, and this leads to some restrictions in applications. To remove such restrictions, the ultra-low field MRI approach has been proposed. Because of the loss of sensitivity, the detection methods based on superconducting quantum interference devices (SQUIDs) in a shielded room were used. Atomic magnetometers have similar sensitivity as SQUIDs and can also be used for MRI, but there are some technical difficulties to overcome. We demonstrate that MRI of the human brain can be obtained with an atomic magnetometer with in-plane resolution of 3 mm in 13 min. © 2013 AIP Publishing LLC.

[<http://dx.doi.org/10.1063/1.4816433>]

Magnetic resonance imaging (MRI) is a valuable radiation-free diagnostic method based on nuclear magnetic resonance (NMR) that provides high contrast to soft tissues and anomalies. In MRI, the signal is magnetic field generated by precessing nuclear spins, in most cases protons. Their precession frequency is determined by a DC magnetic field. The proton density in tissues is imaged with the help of frequency and phase-encoding field gradients that disperse frequencies and phases of the contributions coming from different areas of the object. The DC field serves two purposes: to polarize the nuclear spins and to set NMR frequency.

Because the signal-to-noise ratio (SNR) and image quality improve with the field strength, conventional clinical scanners use fields as high as 3 T. This, however, leads to various restrictions in applications due to high price, lack of mobility, and need for cryogenics. Ultra-low field (ULF) MRI is a promising alternative method that can remove many restrictions of high-field systems. In particular, ULF MRI scanners can be constructed at much lower cost, can be much lighter, and can have many other useful features such as higher contrast to anomalies, absence of susceptibility artifacts, and compatibility with other systems. Unfortunately, the SNR is reduced due to lower nuclear polarization and detector sensitivity.

The low SNR problem is partially solved with the use of strong prepolarization fields (B_p). This field is turned on during the prepolarization cycle to create enhanced nuclear polarization that lasts for several T_1 times (longitudinal spin-relaxation times) and is turned off during the measurement cycle. During this cycle only the uniform and stable ULF field (B_m) remains that defines the NMR frequency. The uniformity of B_p is not particularly important, so compact and efficient magnet systems can be constructed to generate a strong B_p field, but the need to remove rapidly the B_p field precludes the use of ferromagnetic materials. Coils have been the only option for B_p in the system designed for anatomical imaging. The B_p coils can produce the fields on the order of 0.1 T that can be removed in 20–60 ms. Note that in the case of high-field MRI one field has the functions of B_p and B_m , so it has to be highly uniform, which is not easy to achieve.

Detector sensitivity at ULF, which is also quite poor, has been improved by replacing room-temperature coils with superconducting interference devices (SQUIDs), by installing the system inside a shielded room, by using Litz-wire B_p coils, and by employing gradiometers. With these measures, the sensitivity has become sufficient for imaging the human brain at ULF.¹ The emerging technology of high-sensitivity atomic magnetometers (AMs) that rival SQUIDs in sensitivity can be a good alternative, with the important advantage of non-cryogenic operation. Indeed, several publications demonstrated that AMs can be used to image not only phantoms² and liquid flows³ but also anatomy.⁴ However, anatomical MRI of the human brain, or a similar large object, has not been yet demonstrated with AMs. Such demonstration constitutes the main goal of the current letter.

One problem in applications of AMs to MRI is that magnetic field and gradients applied during the data acquisition cycle negatively affect the operation of the AM.² The MRI DC field “detunes” the AM from the NMR frequency, while the MRI gradients broaden the AM magnetic resonance, reducing its sensitivity. At least three solutions have been previously explored: a remote detection,³ an offset of the AM field with a solenoid,^{5,6} and the decoupling of fields and gradients with a flux transformer (FT).⁷ The last solution is most practical for anatomical imaging and is used in the current work.

An FT is a set of two connected coils, one to receive the MRI signal from the imaged object (input coil) and the other (output coil) to generate the field from the current driven by the first coil. In the FT+AM system, the output coil is positioned in the vicinity of the AM. The FT can be cryogenic, as in SQUID systems, or non-cryogenic, as in our AM-based setup, which is desirable for constructing fully non-cryogenic systems. The non-cryogenic FT removes the DC component and suppresses low-frequency spectral components of the signal, while passing the AC component at the frequency of interest. Some losses in SNR are present due to intrinsic Johnson noise of room-temperature conductors, but these losses can be reduced by increasing frequency.⁷

The principle of operation of the current ULF MRI system is the same as in Ref. 4. Initially the B_p field is turned on

to prepolarize spins and then is switched off before the MRI sequence begins. After some delay, needed for settling transients generated by the B_p , a $\pi/2$ -pulse is applied to start nuclear precession. Then phase encoding gradients are applied to set the phase of the signal, and a π -pulse is applied to reverse phase evolution of spins and remove the effects of external gradients. Time intervals are optimized for image quality. B_p is turned on at zero time and turned off at $t_p = 450$ ms; the $\pi/2$ -pulse is applied at $t_p + 63$ ms; the gradient pulses are turned on at $t_p + 69$ ms for 35 ms; the π -pulse is applied at $t_p + 100$ ms. The acquisition starts after the echo pulse and last for about 100 ms. One phase encoding step takes 800 ms, and the total scan 13 min.

Our non-cryogenic ULF MRI setup and FT+AM detection system⁴ have been redesigned for brain imaging. The current much larger ULF MRI coil system and the modified FT+AM detection system are shown in Fig. 1. The ULF MRI coil system consists of the B_m coil to produce a uniform MRI field of ~ 4 mT, the B_p coil to generate a prepolarization field of 80 mT, and gradient coils to generate frequency and phase-encoding gradients for 3D imaging, as well as to shim parasitic first-order gradients. The B_m coil is driven by a stable current source, which is configured to recover in a short time from the B_p pulses.

The FT-AM operation principles are given in Ref. 7. We have modified the input and output coils of the FT to make

them optimal for brain imaging. Currently, the input coil of the FT has been constructed from two adjacent circular coils of 7 cm diameter connected in sequence to function as a first-order planar gradiometer. The input gradiometer was placed inside the bore of the ULF MRI system at the bottom of the imaged objects. The gradiometer configuration of the input coil reduces external noise and transients from other coils. The sensitivity depth of the gradiometer is about 4 cm, and the field of view (FOV) is about 7 cm. The depth and FOV can be increased by increasing the size of the input coils, but SNR will be decreased inversely with the size. The output coil of FT consists of two coils attached to opposite sides of the AM oven. The detection frequency was chosen as 131 kHz. The AM was tuned to this frequency by a bias field that was generated with a solenoid installed inside the ferrite shield. The AM cell, a glass cell filled with K, N_2 at 50 mTorr, and He at 600 Torr, has been heated to 180 °C with an electrical heater. The heater was electronically turned on during the B_p cycle and turned off during the measurement cycle.

The brain scan took about 13 min with 65 and 15 phase encoding steps in the horizontal and depth directions, respectively. Although the quality could have been improved with longer scans, this time was chosen as practically reasonable for medical applications. A volunteer was lying on the back with the head propped against the G-10 sheet to which the input gradiometer had been attached. In this position, the back part of the head was imaged. Other head positions are also possible to image other parts of the head. The resulting images of the six most informative consecutive coronal slices are shown in Fig. 2. The images reveal some pronounced brain features, brain boundaries, and sulci. Some asymmetry is observed due to a slightly tilted position of the head. The in-plane resolution is 3 mm by 3 mm, similar to that obtained with SQUIDS.¹

Although the demonstrated image quality is certainly inferior to that typical in high-field MRI, it can be sufficient for some niche applications where high resolution is not critical. The quality can also be improved in the future by

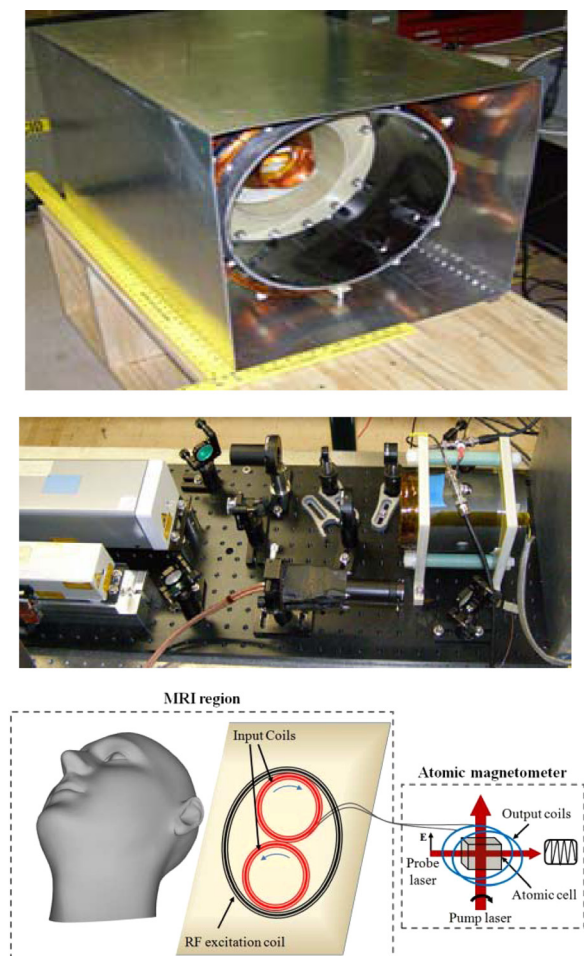


FIG. 1. The ULF-MRI coil system (top) and the AM+FT detection system (middle and bottom) used for brain imaging.

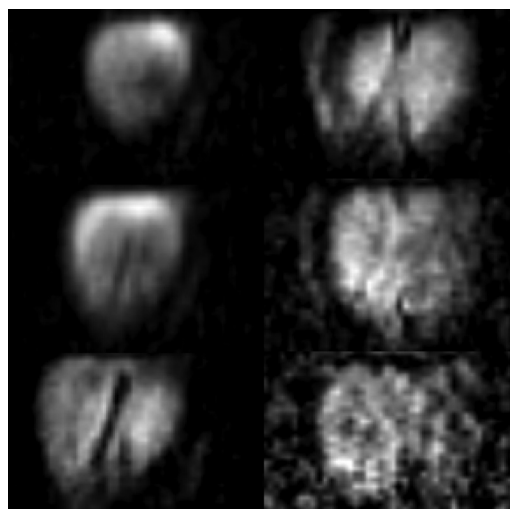


FIG. 2. ULF MRI images obtained with AM: the in-plane resolution 3 mm; slice thickness 5 mm; depths from the top to bottom and left to right 5, 10, 15, 20, 25, 30 mm; field of view about 100 mm; scan time 13 min; prepolarization time 450 ms; acquisition time 100 ms.

increasing the prepolarization field, optimizing MRI sequences, and improving the sensitivity of the detection system. In the current experiment, B_p field was only 80 mT, but much stronger fields are possible to generate by increasing power and adding forced-air cooling. In terms of sequence optimization, with some dynamic field compensation measures, the delay time of the $\pi/2$ -pulse can be reduced from current 63 ms to 20 ms. The brain signal decays very fast (~ 100 ms in the ULF regime),^{1,8} and this reduction in delay can lead to a gain in SNR of ~ 2 times. In addition, it is possible to use other sequences than the current spin-echo sequence to reduce the time between the $\pi/2$ -pulse and the acquisition window. The detection sensitivity can be improved by increasing detection frequency, optimizing geometry, using multi-channel acquisition, and cooling the FT. Some image processing algorithms can also help to reduce noise and improve visibility. A scan can be also made longer to improve SNR. With these measures, the resolution can be improved to 1-2 mm, and full-head coverage can be achieved so that the image quality can become suitable for many clinical applications.

We anticipate that our system will find niche medical applications where high field systems are restricted. For example, the system can be brought into an intensive care unit for taking images of head trauma or other injuries from patients without need to relocate them to MRI facility. This is important because the relocation is dangerous, especially

when life support system needs to be connected. The system can be also used for follow up studies of disease and effects of treatment at lower cost. Besides this, because the system is portable and self-sufficient, without for example need for cryogenics, it can be used in battlefields, in submarines, on ships, etc. Owing to low price, the system can be used for research, for training students, in industry, and in other situations where cost reduction is essential.

This work was supported by NIH 5 R01 EB009355. The work of T. Karaulanov was partially supported by the U. S. Department of Energy through the LANL/LDRD program.

¹V. S. Zotev, A. N. Matlashov, P. L. Volegov, I. M. Savukov, M. A. Espy, J. C. Mosher, J. J. Gomez, and R. H. Kraus, Jr., *J. Magn. Reson.* **194**, 115–120 (2008).

²I. M. Savukov and M. V. Romalis, *Phys. Rev. Lett.* **94**, 123001 (2005).

³S. Xu, V. V. Yashchuk, M. H. Donaldson, S. M. Rochester, D. Budker, and A. Pines, *Proc. Natl. Acad. Sci. U.S.A.* **103**, 12668–12671 (2006).

⁴I. Savukov and T. Karaulanov, *J. Magn. Reson.* **231**, 39–43 (2013).

⁵I. M. Savukov, S. J. Seltzer, and M. V. Romalis, *J. Magn. Reson.* **185**, 214–220 (2007).

⁶V. V. Yashchuk, J. Granwehr, D. F. Kimball, S. M. Rochester, A. H. Trabesinger, J. T. Urban, D. Budker, and A. Pines, *Phys. Rev. Lett.* **93**, 160801 (2004).

⁷I. M. Savukov, V. S. Zotev, P. L. Volegov, M. A. Espy, A. N. Matlashov, J. J. Gomez, and R. H. Kraus, Jr., *J. Magn. Reson.* **199**, 188–191 (2009).

⁸V. S. Zotev, A. N. Matlashov, I. M. Savukov, T. Owens, P. L. Volegov, J. J. Gomez, and M. A. Espy, *IEEE Trans. Appl. Supercond.* **19**, 823–826 (2009).